

ORIGINAL ARTICLE

Within-eye and between-subject variability for reflectance of the retinal nerve fibre layer

Hin Cheung | William H. Swanson  | Brett J. KingIndiana University School of Optometry,
Bloomington, Indiana, USA**Correspondence**William H. Swanson, Indiana University
School of Optometry, Bloomington, IN, USA.
Email: wilswans@indiana.edu**Funding information**National Eye Institute, Grant/Award Number:
R01EY024542**Abstract**

Purpose: Reflectance of retinal nerve fibre layer (RNFL) can contribute to detecting the presence of glaucomatous damage and defining its extent. As a step towards developing a normative database for RNFL reflectance, we assessed within-eye and between-subject variability for RNFL reflectance in healthy eyes.

Methods: Vertical $30^\circ \times 15^\circ$ volume scans at the optic disc were gathered using SD-OCT (Spectralis OCT) from people free of eye disease. Scans were gathered for both eyes of 30 younger adults (mean \pm SD = 27 ± 3 years) and for one eye of 30 older adults (68 ± 8 years). Reflectance was quantified for each voxel as the depth-resolved attenuation coefficient (AC). Values for AC were extracted for four slabs (0–52, 24–52, 24–36 and 36–60 μm) and at depths from 24 to 60 μm below the inner limiting membrane (ILM) in 4 μm steps.

Results: Between-subject and within-eye standard deviations (SDs) for the logarithm of AC were similar; median differences were 0.02–0.03 log unit across all four slabs and depths from 24 to 48 μm . Means for the logarithm of AC were higher for younger than older eyes by ~ 0.1 log unit; this age effect was not due to differences in the raw reflectance of the RNFL, but rather to age-related changes in reflectance of deeper retina affecting the calculation of AC.

Conclusions: In both groups, within-eye variability in RNFL reflectance near the optic disc was similar to between-subject variability. A better understanding of within-eye variability would be useful for developing normative databases.

KEYWORDS

between-subject variability, en face images, reflectance, retinal nerve fibre layer, within-eye variability

INTRODUCTION

Measurement of retinal nerve fibre layer thickness (RNFL) with optical coherence tomography (OCT) has contributed substantially to the management of patients with glaucoma but has been limited by high between-subject variability in normal eyes. For circumpapillary RNFL thickness,

there is overlap in distributions between healthy eyes and eyes with damage.^{1–3} One aspect of this is biological variability, such as the two-fold difference in the normal variation of RNFL thickness, ganglion cell and axon counts.^{4–8} Another aspect is variability caused by artefacts due to choice of measurement, such as the effects of axial length for global circumpapillary RNFL thickness and location of

This is an open access article under the terms of the [Creative Commons Attribution-NonCommercial-NoDerivs](https://creativecommons.org/licenses/by-nc-nd/4.0/) License, which permits use and distribution in any medium, provided the original work is properly cited, the use is non-commercial and no modifications or adaptations are made.

© 2022 The Authors. *Ophthalmic and Physiological Optics* published by John Wiley & Sons Ltd on behalf of College of Optometrists.

the major blood vessels for sector thicknesses. A related artefact from the choice of measurement is in en face RNFL thickness deviation maps, where arcuate defects occur in about 20% of eyes free of glaucoma⁹ due to normal between-subject variability in the distance from the fovea to the arcades.^{10,11}

Several laboratories have reported that en face maps of RNFL reflectance show good potential for detecting glaucomatous damage,^{12–19} and that by using fixed distances below the inner limiting membrane (ILM) the problems with normal between-subject variability in the distance from the fovea to the arcades can be avoided.^{20,21} Measured reflectance will be affected by factors that reduce the amount of light that reaches the tissue, such as shadows from blood vessels or floaters and changes in the position of the eye, but not by factors that affect RNFL thickness such as axial length. Methods have been developed to reduce these effects by estimating an ‘attenuation coefficient’ (AC), which calculates the amount of light attenuated at a given voxel by comparing its measured reflectance with reflectances measured at voxels below it.^{22–24} This study is designed to explore factors affecting variability in RNFL AC values, which have not yet been studied with the same level of scrutiny that has been applied to variability in RNFL thickness values. The goal is to assess biological variability and identify potential artefacts due to the choice of measurement. One of the strengths of perimetry and RNFL thickness as complementary clinical measures is that they typically have different sources of artefact. To the extent that the sources of variability are different for RNFL reflectance than for RNFL thickness, reflectance may be able to add additional information to clinical evaluation.

Most studies of RNFL reflectance have been performed near the optic disc.^{12–16,19,24,25} Some key factors that affect variability in clinical measures used in patients with glaucoma are axial length and location of major blood vessels for RNFL thickness, age and within-subject variability for perimetry. Age has been found to cause a decline in AC,¹⁵ and within-subject variability in AC has been noted for locations around the optic disc.^{15,19} This study compared within-eye and between-eye variability in a region temporal to the disc, and explored the effects of age and axial length. Effect sizes were evaluated in terms of logarithmic differences in means and SD, and the square of the correlation coefficient. There were no tests of statistical significance, so sample size was set to 30 per group to allow relatively unbiased estimates of SD in groups small enough to allow ready replication.¹¹

METHODS

Participants

Volume scans were analysed for two groups of 30 people each. The first group had been chosen as age-similar sex-matched controls for a separate study²⁶ of 30 patients with

Key points

- En face maps of retinal nerve fibre layer reflectance are relatively unaffected by factors that have a substantial impact on measures of retinal nerve fibre layer thickness.
- Reflectance maps have potential to provide a clinically useful addition to measures of retinal nerve fibre layer thickness, so population norms should be valuable.
- Key factors when gathering population norms for retinal nerve fibre layer reflectance are effects of the shape of the eye, retinal region studied and the diversity of the subjects recruited.

TABLE 1 Age, axial length and circumpapillary RNFL thickness for younger and older groups

	Younger left	Younger right	Older
<i>n</i>	30	30	30
Age in years (mean ± SD)	27 ± 2.7	Same as left eye	68 ± 8.3
Axial length in mm (mean ± SD)	24.2 ± 1.0	24.3 ± 1.0	24.2 ± 1.1
Axial length range	22.5 to 27.0	22.5 to 27.2	22.2 to 26.5
RNFL thickness in µm (mean ± SD)			
Global	99 ± 9	99 ± 10	96 ± 7
Superior temporal	134 ± 19	141 ± 20	135 ± 14
Inferior temporal	140 ± 19	141 ± 22	138 ± 15

glaucoma, resulting in 17 males and 13 females in the age range of 52 to 78 years. Each person in this group had been imaged on one eye only, which had been selected as their study eye in the original investigation. Then 17 males and 13 females were selected from a pool of 60 young adults imaged for a published study.¹¹ The age range for this group was 22 to 33 years, and that study imaged both eyes. See Table 1 for descriptive statistics for age, axial length and circumpapillary RNFL thickness.

Inclusion and exclusion criteria

Common inclusion criteria for both groups were best-corrected visual acuity of logMAR 0.30 (6/12) or better, refractive corrections between +3.00 and –6.00 dioptre spherical equivalent, cylinder no more than 3.00 dioptres, clear ocular media and the absence of known eye disease during a comprehensive eye examination within the past 2 years.

Common exclusion criteria for both groups were ocular or systemic disease that was currently affecting visual function (e.g., diabetic retinopathy, prior arterial or vein occlusion, macular degeneration, glaucoma); a history of intraocular surgery (except uncomplicated cataract surgery more than 1 year before enrolment); usage of medications known to affect vision; recent intraocular pressure (IOP) greater than 20 mmHg; narrow angles; OCT scans with low image quality or high segmentation errors and eyes with epiretinal membranes seen on en face imaging.

Imaging protocol

Informed consent was obtained from each participant after an explanation of the procedures and goals of the study and prior to testing. This study adhered to the tenets of the Declaration of Helsinki and was approved by the Institutional Review Board at Indiana University. Scans of our subjects were acquired for other studies using a spectral domain OCT system (Spectralis; Heidelberg Engineering, heidelbergengineering.com). A $30^\circ \times 15^\circ$ vertical rectangular scan centred on the optic disc was acquired using high-speed mode, vertical b-scans with $30 \mu\text{m}$ spacing and automatic real-time function (ART) averaging across 9 images, see [Figure 1](#). Axial length measurements were also collected previously (IOLMaster 500; Carl Zeiss Meditec, zeiss.com).

Selection of the retinal region for evaluation

A pilot study measured AC as a function of depth below the ILM at a wide range of locations across the retina within 15° from fixation in five older adults free of eye disease. The same pattern was seen in all five eyes, an example is shown in [Figure 1](#) (upper panels). For all regions of interest (ROIs), AC had an initial steep increase from the ILM to $12 \mu\text{m}$ below it, then increased more slowly before declining after reaching the bottom of the RNFL. The AC at $16 \mu\text{m}$ below the ILM (indicated by the vertical dashed line in the upper right panel) was lowest at the fovea where the RNFL is absent. The next lowest values were in the temporal raphe where fibres are less densely packed. Peak AC was greatest in the parafoveal region, the arcades and near the optic disc. Only for regions near the disc was the RNFL thick enough that AC had not always begun to decline by $60 \mu\text{m}$ below the ILM. The AC at $16 \mu\text{m}$ below the ILM showed a 5-fold range with location across the central retina, compared to a 2-fold range near the optic disc. Therefore, in order to look at the greatest range of distances below the ILM and reduce within-subject variability, for this study the emphasis was on locations near the optic disc as shown in the lower panels of [Figure 1](#).

Image processing and data extraction

Methods for generating AC maps and local logAC values have been published previously.²⁵ Briefly, scans were processed using custom MATLAB (R2018a; MathWorks, mathworks.com) software to generate AC maps using Equation 17 in Vermeer et al.²² The initial analysis was for a vertical column of 14 circular ROIs with a radius of 15 pixels (0.6° of visual angle) near the temporal edge of the image (between the fovea and the optic disc), ensuring that both superior and inferior temporal bundles were included. Care was taken to avoid parts of the image that may cause potential artefacts, such as major blood vessels or noise in the image. The four ROIs overlying the papillomacular bundles fell below the RNFL at deeper depths and were excluded from analysis of within-eye differences, leaving five ROIs each sampling the superior temporal and inferior temporal RNFL bundles.

The manual method of placement can avoid blood vessels and other sources of artefacts, but could introduce a source of bias, even something as subtle as the amount of displacement left and right when choosing a column to avoid blood vessels. To assess effects of such bias, a second method used spatial filters to segment out the major blood vessels and automated placement of a grid of locations. Each grid element was a square 30 by 30 pixels, so that the width of a square was the same as the diameter of the circles in the manual method. Two 7×3 rectangular sets of grid elements for superior and inferior disc sectors were used to assess within-subject differences, which corresponded to regions sampled by the two sets of five ROIs for the manual method. The lower left panel of [Figure 1](#) shows the two rectangles superimposed on an example of 14 ROIs. The three horizontal positions span the range of horizontal positions used in the manual placement. This method has a potential source of artefact: insufficiently avoiding blood vessels would yield an increase in the AC.

For each circular ROI or grid element, the arithmetic mean for AC across voxels was computed, shown as a function of depth below the ILM in the lower right panel of [Figure 1](#) for the 14 circular ROIs. The arithmetic mean was chosen for averaging across voxels, because a few voxels with extreme values for AC would have a smaller impact for an arithmetic mean (averaged in linear units) than for a geometric mean (averaged in log units). However, the descriptive statistics for the ROIs and grid elements were performed in log units because SD in log units is independent of the mean and our primary goal was to compare within-eye and between-subject variability.

Analysis

In order to assess the extent to which logAC and RNFL thickness are independent measures, we estimated the average thickness for each ROI by finding the depth at which

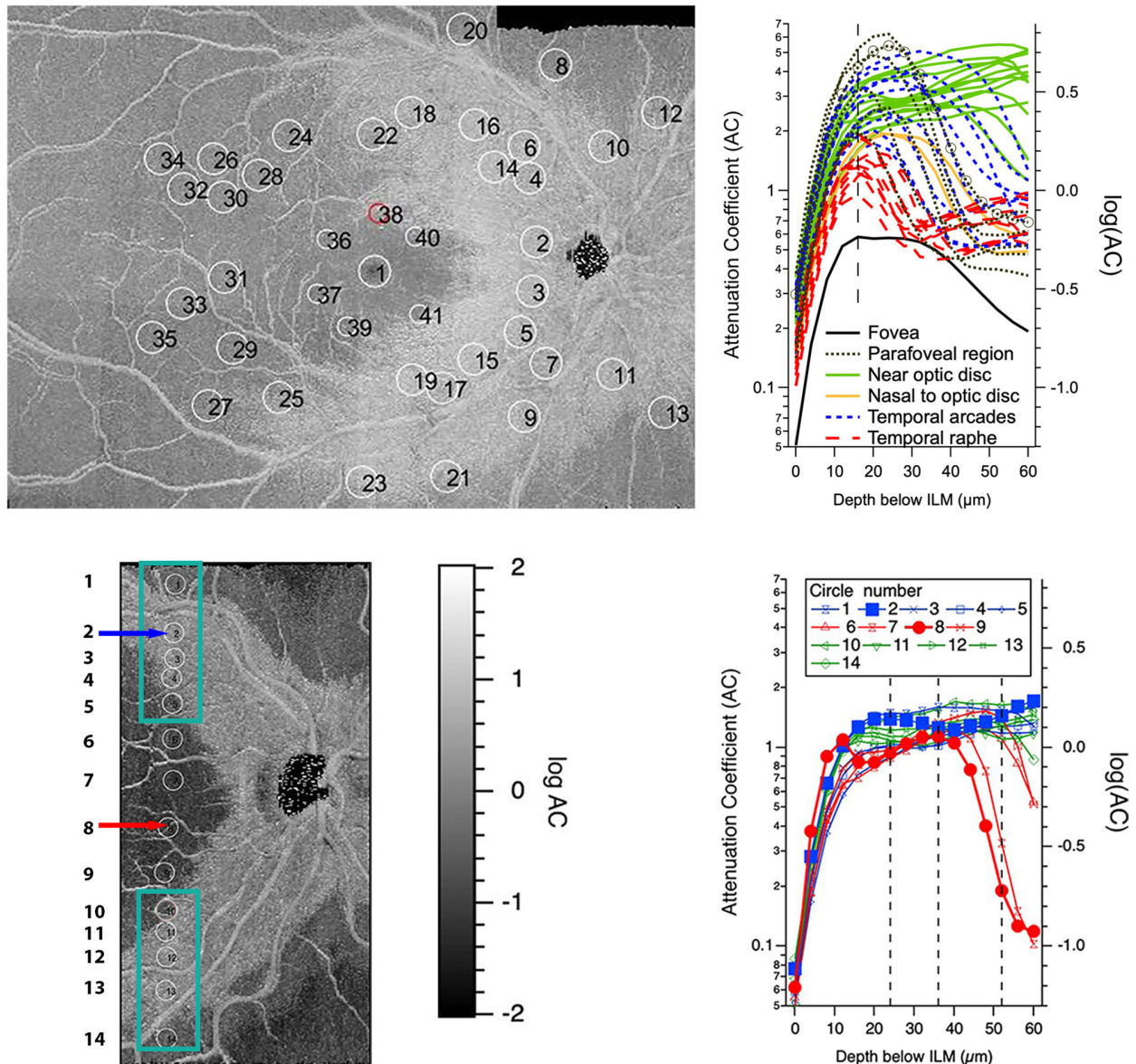


FIGURE 1 Examples of measurement of attenuation coefficient (AC) for individual eyes of older controls. *Upper left*: AC values at 40 μm below the inner limiting membrane (ILM) at 41 locations within 15° of the fovea for one older control. Higher AC is found at retinal areas with higher retinal nerve fibre layer (RNFL) density and lower AC is found in the temporal raphe where distinct spaces between fibre bundles can be seen as darker, less reflective areas. *Upper right*: AC versus depth below the ILM for these 41 locations in this one older control, grouped by retinal region as indicated in the legend. The parafoveal function shown with dotted black lines and small black circles indicates the AC values for location 38 (with the red circle to the left). The vertical dashed line indicates a depth of 16 μm . *Lower left*: Regions of interest (ROIs) near the disc evaluated in this study in another older control, on a 30° × 15° AC map at 76 μm below the ILM where the vasculature can be readily visualised. Circles show 14 ROIs manually placed near the temporal edge of the image while avoiding large-calibre vessels, numbered from top to bottom. The blue and red arrows indicate ROIs 2 and 8, data for which are highlighted in the lower right panel. Blue rectangles show the corresponding regions analysed with the automated method. *Lower right*: AC plotted as a function of depth from the ILM for the ROIs numbered on the lower left. Solid symbols are for the two ROIs with the smallest (8, red circles) and greatest (2, blue squares) RNFL thickness. Vertical dashed lines indicate depths of 24, 36 and 52 μm from the ILM, which were used for computing slabs. The curves shown in red are for the locations that were not used in analysis of within-subject variability because they typically fell below the RNFL by 60 μm below the ILM.

AC declined from the peak at prior depths by a criterion amount that was varied from 0.0 to 0.3 log unit in 0.1 log unit steps. The criterion of 0.0 log unit identified the depth with peak AC value, the criterion of 0.3 log unit identified the depth at which AC fell to half of the peak and the other two criteria identified the depths at which AC fell to 79% and 63% of the peak value. For each criterion amount, the

correlation was computed between log AC and thickness across all 420 ROIs (14 each for 30 eyes). Then, R^2 was used as a measure of dependence.

Variability and age effects were evaluated in terms of slabs (AC averaged across a range of depths below the ILM) and at individual depths. Slabs averaged AC at depths 0–52, 24–52, 24–36 and 36–60 μm below the ILM. Individual

depths ranged from 24 to 60 μm below the ILM in 4 μm steps. We noted previously that superficial gliosis occurring in older eyes usually disappears by 24 μm below the ILM.²⁷ Likewise, specular reflections occurring in younger healthy eyes usually disappear by the same depth. Mean and SD for logAC were calculated for the four slabs and 10 depths. Data were analysed separately for left and right eyes for the younger adults, with the expectation that the means and SD would be very similar. Data for one eye per person were analysed for the older adults. The separate analyses for two eyes for the younger group provide a way to assess the effective magnitude of any age effect. If the difference in a measure between the younger and older groups is smaller than the difference in the measure between the two eyes of the younger group, then any age effect on the measure is not likely to be substantial.

For each slab and depth, the within-eye difference for each eye was computed as the difference in mean logAC for the superior and inferior regions and the average logAC value for the eye was computed by averaging the logAC values for these two regions. Within-eye variability in each group of eyes was computed as the SD of the difference across the 30 eyes in the group. Between-subject variability was computed as the SD for average logAC value across the 30 eyes. Age effect was evaluated by comparing the average logAC values for younger and older eyes. The correlation between axial length and average logAC values was used to assess the impact of axial length, with R^2 as a measure of effect size. Data were also evaluated when disaggregated by sex because of the United States National

Institutes of Health (NIH) requirement to consider sex as a biological variable, even though there is no evidence of sex differences in the literature.

RESULTS

Manual placement of regions of interest

Results for the left eyes of the younger adults for all 14 ROIs are shown in Figure 2. Across all eyes and circles, individual values for AC ranged from -0.4 to $+0.7$ log unit, as illustrated in the left panel. When averaged across individuals in a group, mean AC differed by about 0.1 log unit across circle locations, as shown in the middle panel; for most locations, AC was about 0.1 log unit lower for the older eyes. When averaged across all circles for an individual, mean AC differed across individuals by ~ 0.5 log unit, as shown in the right panel.

The comparison of logAC and RNFL thickness found that they were relatively independent, with $R^2 < 1\%$ for all four criteria, for both left and right eyes of the younger controls.

To compare standard deviations (SDs) for within-eye and between-subject differences, analysis was restricted to the 10 ROIs used for the superior and inferior retina. SDs are shown for all depths and slabs in Table 2; Figure 3 shows an example for a depth of 24 μm below the ILM. Means for within-eye differences were 0.01 to 0.03 log unit, as illustrated by the horizontal dashed lines. There was an 0.4–0.5 log unit range of differences across most of the range of

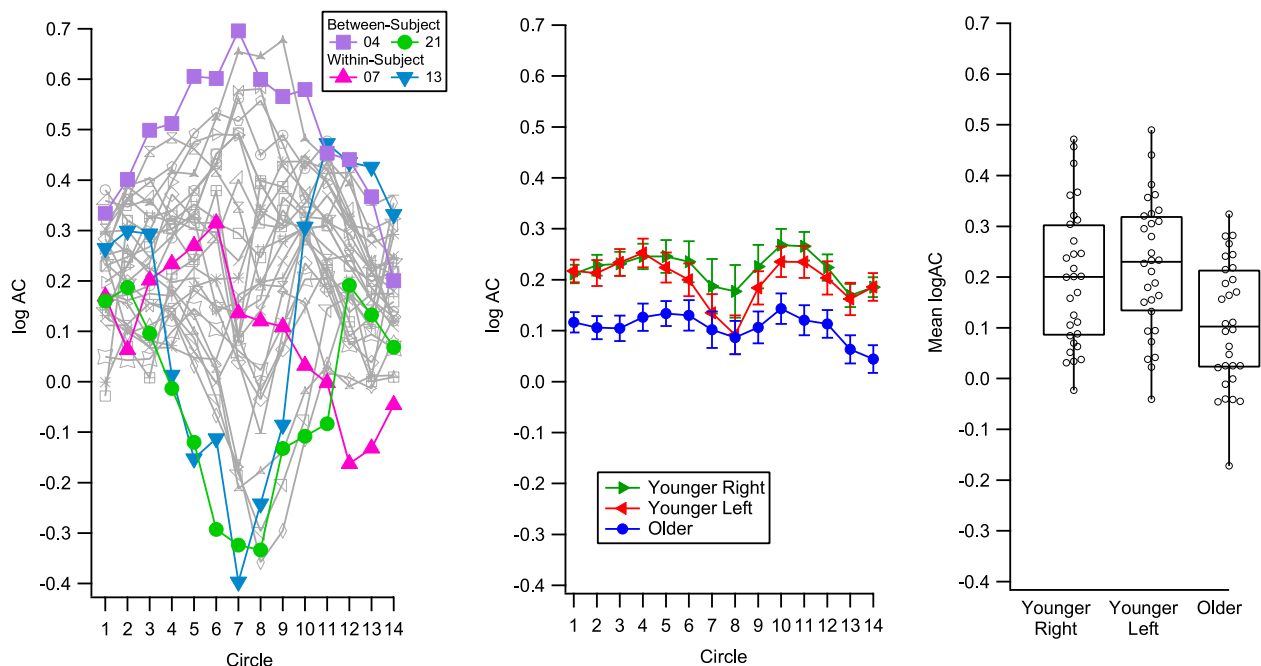
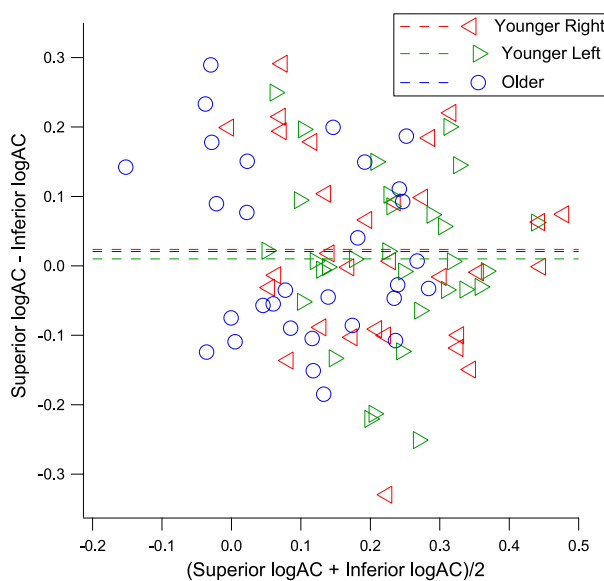


FIGURE 2 Results from manual placement of the 14 ROIs at 24 μm below the inner limiting membrane (ILM). Left panel illustrates the variability for the left eyes of the younger adults by showing results for every circle. (Refer to [supplementary material](#)) Coloured symbols show examples as indicated in the legend, illustrating extremes for between-subject variability (04 and 21) and within-subject variability (07 and 13). Middle panel shows the means for each of the circles for the three groups; error bars show \pm one standard error of the mean. Right panel shows box and whisker plots for the mean of the 14 circles for each subject per group, where the box shows the interquartile interval and whiskers show the full range.

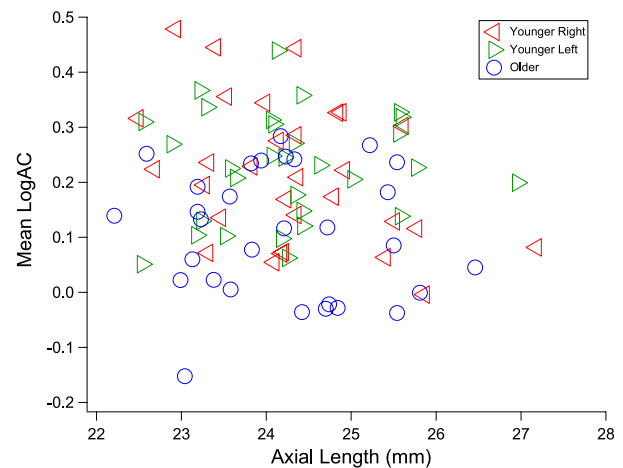
TABLE 2 Standard deviations in log units for between-subject differences and within-eye differences for the three groups

	Younger left		Younger right		Older	
	Between	Within	Between	Within	Between	Within
Slab						
0–52 μm	0.14	0.13	0.16	0.15	0.14	0.13
24–52 μm	0.15	0.12	0.16	0.14	0.14	0.13
24–36 μm	0.15	0.13	0.16	0.14	0.15	0.13
36–60 μm	0.16	0.13	0.16	0.16	0.15	0.13
Depth						
24 μm	0.14	0.12	0.16	0.14	0.14	0.13
28 μm	0.15	0.12	0.16	0.13	0.15	0.13
32 μm	0.15	0.13	0.16	0.13	0.15	0.13
36 μm	0.15	0.12	0.17	0.14	0.15	0.13
40 μm	0.15	0.12	0.17	0.14	0.15	0.13
44 μm	0.15	0.12	0.17	0.15	0.15	0.13
48 μm	0.16	0.12	0.17	0.16	0.15	0.13
52 μm	0.19	0.13	0.18	0.18	0.16	0.13
56 μm	0.24	0.14	0.21	0.20	0.18	0.15
60 μm	0.29	0.16	0.26	0.21	0.22	0.16

**FIGURE 3** Within-eye variability at 24 μm below the inner limiting membrane (ILM). The difference in logAC values for circles 1–5 (superior) and for circles 10–14 (inferior) is shown versus the mean of these values. Horizontal dashed lines show the mean differences for the three groups.

mean values. For all three groups of eyes, SDs were similar for within-eye and between-subject differences. For all depths and slabs, the median differences between SDs were 0.02 to 0.03 log unit. SDs were not higher for the older eyes.

As shown in Figure 4 and Table 3, the effects of axial length were minor, with values of R^2 for the 10 depths ranging from 1% to 16% for the younger eyes and not greater

**FIGURE 4** Mean logAC at 24 μm below the inner limiting membrane (ILM) as a function of axial length. Mean values are for the 10 circles used in Figure 3.

than 1% for the older eyes. The effects of sex as a biological variable were minor. Differences in average logAC between males and females were no greater than 0.06 log unit across all slabs and depths, and were not consistent across groups. Mean log AC was slightly lower for males for the older eyes and the left eyes of the younger group, but was slightly higher for males for the right eyes of the younger group.

Automated removal of blood vessels

Across all depths and slabs, the within-eye SDs for the automated method were 0.00 to 0.03 log unit larger than for

TABLE 3 R^2 values for correlation of logAC with axial length

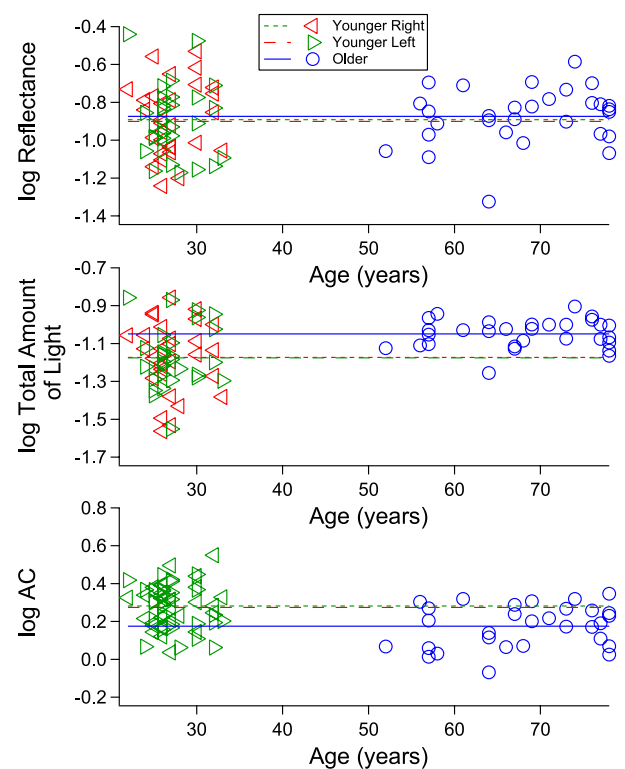
	Younger left (%)	Younger right (%)	Older (%)
Slab			
0–52 μm	1	18	0
24–52 μm	1	15	0
24–36 μm	1	17	1
36–60 μm	4	10	0
Depth			
24 μm	1	16	1
28 μm	1	16	1
32 μm	0	15	1
36 μm	0	14	0
40 μm	1	14	0
44 μm	1	13	0
48 μm	2	11	0
52 μm	3	8	0
56 μm	6	4	0
60 μm	9	4	0

TABLE 4 Amount in log units by which mean logAC was larger for the automated method than the manual method

	Younger left	Younger right	Older
Slab			
0–52 μm	0.13	0.13	0.15
24–52 μm	0.05	0.05	0.05
24–36 μm	0.05	0.06	0.06
36–60 μm	0.07	0.05	0.05
Depth			
24 μm	0.04	0.06	0.06
28 μm	0.04	0.06	0.06
32 μm	0.03	0.06	0.06
36 μm	0.03	0.05	0.05
40 μm	0.03	0.04	0.05
44 μm	0.04	0.04	0.04
48 μm	0.04	0.05	0.03
52 μm	0.05	0.05	0.03
56 μm	0.07	0.06	0.03
60 μm	0.09	0.09	0.05

the manual method, and the between-subject SDs were within ± 0.03 log unit for the two methods. For the means, the values for the automated method were 0.03 to 0.15 log unit larger than for the manual method; as shown in Table 4, the largest differences were for the 0–52 μm slab and the 60 μm depth. The primary findings were almost identical to results with the manual method: mean log AC was ~ 0.1 log unit lower for the older eyes than the younger eyes, and the within-eye SDs were similar to the between-eye SDs.

The automated method was used to assess age effects in terms of the measured reflectance for a voxel and an estimate of the total amount of light arriving at the voxel based on reflectance measured at depths below the voxel. The AC is computed from the reflectance divided by the total amount of light. This means that log AC equals log reflectance minus log total amount of light. Figure 5 shows the log values at 24 μm below the ILM for reflectance, total amount of light and AC, both for means (horizontal lines) and for individual eyes (symbols) plotted against age. For measured reflectance (top graph), the mean values for the left and right eyes of the younger adults were 0.02 and 0.03 log unit lower than for the older eyes. For the estimate of the total amount of light (middle graph), means were 0.12 and 0.13 log unit lower than for the older eyes while AC (bottom graph) was 0.11 and 0.10 log unit larger than for the older eyes. This indicates that the age effect seen for AC is due to an age effect on the estimate of total amount of light. The SD for the measured reflectance was 0.19 log unit for both left and right eyes of the younger adults and 0.15 log unit for the older adults. The SD for the total amount of light was 0.19 and 0.16 log unit for the left and right eyes of the younger adults, respectively, and 0.08 log unit for the older adults.

**FIGURE 5** Log values for reflectance (top), total amount of light (middle) and attenuation coefficient (AC) (bottom) for younger and older controls at 24 μm below the inner limiting membrane (ILM) plotted against age. Horizontal lines show the means for the three groups.

DISCUSSION

En face RNFL reflectance maps have been found to have potentially good diagnostic ability for glaucomatous

damage,¹²⁻²⁰ and good agreement with patterns of perimetric loss.^{20,21} Because measured reflectance varies with the amount of light hitting the retina, measures of AC have been developed by using the ratio of measured reflectances for different layers within the retina.²²⁻²⁴ The purpose of this study was to better understand the sources of variability in AC for en face RNFL reflectance maps from healthy eyes. Biological variability in ganglion cell number and in the location of the major blood vessels did not seem to have much effect on RNFL reflectance at 24 μm below the ILM; as shown in [Figures 1 and 2](#), there is relatively little change in AC between ROIs with large differences in RNFL thickness. Furthermore, RNFL thickness explained less than 1% of the variance on logAC. Age had a small impact on AC, and as seen in [Figure 5](#), this seems to reflect an artefact due to the choice of measurement: computation of AC assumes that there is random scattering at levels below the RNFL reflectance, and this may not hold for older eyes. The effect of axial length on between-subject variability of AC was modest, with R^2 values from 0% to 17%. For a sample size of 30, the 95% confidence interval for R^2 includes values as high as 19% when the measured value is 1%, and as small as 0% when the measured value is 17%.

This means that en face RNFL reflectance maps show little effect of biological factors that are known to affect RNFL thickness maps, making it likely that maps of reflectance could be a useful clinical addition to measurements of RNFL thickness. For instance, what appears as an arcuate defect on an RNFL thickness deviation map in a healthy eye⁹⁻¹¹ would not appear as an arcuate defect on a reflectance map. On the other hand, when an arcuate pattern in a thickness deviation map truly reflects glaucomatous damage, it is very likely that it would appear as an arcuate defect in an en face reflectance map. Given this substantial clinical potential, the remainder of this discussion focuses on limitations of what can be concluded from the current data and discussion of what new types of data would be useful.

We found an artefact from choice of measurement: a small decline in mean logAC with age, which was not due to a decrease in the reflectance of RNFL but to an increase in reflectance from deeper layers. A potential explanation is that age-related changes to retinal layers underneath the RNFL increase scattering. For example, the reflectance of the RPE is known to increase with age, presumably due to increasing thickness and decreasing concentration of melanin.^{28,29} An increase in reflectance contributed from outer retinal layers with age would increase the denominator and thereby lower AC. Another factor that could affect AC is defocus, which reduces the reflectance from layers deeper in the retina.²² Such artefacts for depth-resolved AC should be explored in more detail, over wider retinal regions. However, the effect is small and variability did not increase with age. We infer that this issue should be dealt with by measuring age norms for mean AC.

Within-eye and between-subject variability in AC were similar at most depths, with an increase starting at 52 μm , as shown in [Table 2](#). This could be due to individual differences

in RNFL thickness so that for some individuals these deeper depths were at the border between RNFL and the ganglion cell layer. The non-RNFL tissue in these eyes would have lower reflectance and decrease the mean for logAC while increasing the SD. This is the very reason why regions in the papillomacular bundle were removed, to be able to use deeper depths as recommended in a prior study.²⁵ Use of even deeper depths is likely to introduce artefacts due to biological variability in RNFL thickness and the distance from the fovea to the arcades. We infer that it may not be useful to assess reflectance at depths below 52 μm .

We found that AC modestly decreased between-subject variability in mean reflectance ([Figure 5](#)), but there was still a range of ~ 0.5 log unit in each group ([Figure 2](#), right panel). Prior studies have compensated for this by using a within-eye reference value below the RNFL in the temporal raphe to adjust for differences in overall reflectance.^{17,30} This study found that such adjustments may not be sufficient, because of substantial variation across subjects for the magnitude of the within-eye differences among retinal locations for which the mean differences between ACs were small (see [Figure 3](#)). A better understanding of the sources of within-eye variability may be useful to identify ways of reducing the effect of artefacts.

A recent study used azimuthal filtering around the disc to account for individual differences in effects of retinal location on RNFL reflectance, which resulted in an average between-subject SD of 0.18 log unit.¹⁹ This is comparable to the median SD of 0.15 log unit that we obtained using AC as a method for individualising reflectance for an eye. Their method accounted for variations in reflectance due to the angle at which the imaging beam strikes the RNFL, so accounting for effects of shape of the eye could potentially reduce within-subject variability. The effect of axial length was small, with less than 16% of the variance for logAC explained by axial length at any given depth across all eyes. However, the refractive error of our subjects was restricted to between +3.00 and -6.00 dioptre spherical equivalent as part of the inclusion criteria. Within this limited range, high myopes and ultimately eyes with long axial lengths were excluded. Furthermore, axial length does not fully characterise differences in the shape of the eye.³¹ Therefore, we have not assessed the full effects of eye shape in relation to logAC, and future studies should include a wider range of axial lengths.

This study used two different measures, manual placement of ROIs to avoid blood vessels and an automated method that removed pixels affected by blood vessels. Both have different sources of potential bias, yet yielded similar results for the primary findings: within-eye SDs were similar to between-eye SDs, and there was a small age effect for mean logAC. This indicates that the main results are not due to bias in one of the methods. The average values for logAC were slightly larger for the automated method ([Table 4](#)), which is consistent with the latter method not always properly excluding vasculature. Blood absorbs light, which causes the depth-resolved AC

to be over-estimated because it assumes that all light loss is due to scatter. This means that grid elements which included vasculature would have a higher value for AC than other regions, which would cause a modest increase in the mean across the different regions. The fact that the largest difference between the two methods was 0.15 log unit indicates that the automated method is only modestly biased by failing to detect vasculature, and yet there is room for improvement.

This study only looked at ROIs from a vertical column temporal to the optic disc, due to the goal of evaluating within-subject variability at a range of depths within the RNFL. As shown in [Figure 2](#), the mean logAC for each group of eyes showed a relatively small variation across these ROIs. These are also locations where RNFL defects are often found in patients with glaucoma. As shown in [Figure 1](#), a pilot study found that AC at 24 µm below the ILM showed lower variation in regions near the optic disc and provided the greatest range of depths to analyse. Assessment of variability of RNFL reflectance across wider regions of the posterior pole may reveal regions with lower within-subject variability than in the region studied, or perhaps help identify the sources of variability.

This study was not designed to look for the effect of sex; we reported it because the analysis of sex as a biological variable is requested by the US National Institutes of Health. For all depths and slabs, mean logAC for females was slightly higher than for males in the older eyes, but only for the left eyes of the younger group. A much larger sample size would be needed before drawing any conclusions about an interaction between sex and age effects on logAC.

An additional factor to consider in future studies is related to the recruitment of subjects. Most younger adults recruited were students in the optometry or vision science graduate programmes, and older adults were recruited in and around Bloomington, Indiana. Most of our subjects classified themselves 'White, Not Hispanic' with few members of other racial/ethnic groups being represented in this sample. Subjects classified as White have been reported to have slightly lower mean values for RNFL thickness, rim area and disc size than other groups,^{32–35} but there have not been reports on effects on RNFL reflectance. Future studies should include a wider range of socioeconomic groups and increase ethnic diversity.

In summary, we found that RNFL reflectance shows relatively minor impact of the major factors which cause artefacts in RNFL thickness deviation maps, which supports the use of RNFL reflectance as a clinical measure. We have also identified factors that should be addressed when developing population norms to be used clinically: factors affecting within-eye variability such as the shape of the eye and retina region studied, automated removal of blood vessels and a more diverse range of subjects across the lifespan.

AUTHOR CONTRIBUTIONS

Hin Cheung: Conceptualization (equal); data curation (equal); formal analysis (equal); investigation (equal);

methodology (equal); visualization (equal); writing – original draft (lead). **William H. Swanson:** conceptualization (equal); data curation (equal); formal analysis (equal); funding acquisition (lead); investigation (equal); methodology (equal); resources (lead); supervision (lead); visualization (equal); writing – review and editing (lead). **Brett J. King:** Formal analysis (supporting); investigation (supporting); methodology (supporting); supervision (supporting); writing – review and editing (supporting).

ACKNOWLEDGEMENTS

Research reported in this publication was supported by the US National Eye Institute of the National Institutes of Health under award number R01EY024542. The content is solely the responsibility of the authors and does not necessarily represent the official views of the National Institutes of Health. The authors alone are responsible for the content and writing of the paper.

CONFLICT OF INTEREST

Dr Cheung and Dr King and have no potential conflicts of interest to disclose. Dr Swanson: Heidelberg Engineering provided software for the extraction of raw (.vol) image files from the Spectralis OCT used in the study. This software was provided free of charge by the company for use in our research. The company played no other role in the research and has not contributed to the manuscript in any way.

ORCID

William H. Swanson  <https://orcid.org/0000-0003-1331-3658>

REFERENCES

1. Sihota R, Sony P, Gupta V, Dada T, Singh R. Diagnostic capability of optical coherence tomography in evaluating the degree of glaucomatous retinal nerve fiber damage. *Invest Ophthalmol Vis Sci.* 2006;47:2006–10.
2. Springelkamp H, Lee K, Wolfs RC, Buitendijk GH, Ramdas WD, Hofman A, et al. Population-based evaluation of retinal nerve fiber layer, retinal ganglion cell layer, and inner plexiform layer as a diagnostic tool for glaucoma. *Invest Ophthalmol Vis Sci.* 2014;55:8428–38.
3. Virgili G, Michelessi M, Cook J, Boachie C, Burr J, Banister K, et al. Diagnostic accuracy of optical coherence tomography for diagnosing glaucoma: secondary analyses of the GATE study. *Br J Ophthalmol.* 2018;102:604–10.
4. Curcio CA, Drucker DN. Retinal ganglion cells in Alzheimer's disease and aging. *Ann Neurol.* 1993;33:248–57.
5. Curcio CA, Allen KA. Topography of ganglion cells in human retina. *J Comp Neurol.* 1990;300:5–25.
6. Jonas JB, Schmidt AM, Muller-Bergh JA, Schlotzer-Schrehardt UM, Naumann GO. Human optic nerve fiber count and optic disc size. *Invest Ophthalmol Vis Sci.* 1992;33:2012–8.
7. Kerrigan-Baumrind LA, Quigley HA, Pease ME, Kerrigan DF, Mitchell RS. Number of ganglion cells in glaucoma eyes compared with threshold visual field tests in the same persons. *Invest Ophthalmol Vis Sci.* 2000;41:741–8.
8. Maurice C, Friedman Y, Cohen MJ, Kaliner E, Mimouni M, Kogan M, et al. Histologic RNFL thickness in glaucomatous versus normal human eyes. *J Glaucoma.* 2016;25:447–51.
9. Leung CK, Lam S, Weinreb RN, Liu S, Ye C, Liu L, et al. Retinal nerve fiber layer imaging with spectral-domain optical coherence tomography: analysis of the retinal nerve fiber layer map for glaucoma detection. *Ophthalmology.* 2010;117:1684–91.

10. La Bruna S, Rai A, Mao G, Kerr J, Amin H, Zemborain ZZ, et al. The OCT RNFL probability map and artifacts resembling glaucomatous damage. *Transl Vis Sci Technol.* 2022;11:18. <https://doi.org/10.1167/tvst.11.3.18>
11. Swanson WH, King BJ, Horner DG. Using small samples to evaluate normative reference ranges for retinal imaging measures. *Optom Vis Sci.* 2019;96:146–55.
12. Fortune B, Burgoyne CF, Cull G, Reynaud J, Wang L. Onset and progression of peripapillary retinal nerve fiber layer (RNFL) retardance changes occur earlier than RNFL thickness changes in experimental glaucoma. *Invest Ophthalmol Vis Sci.* 2013;54:5653–61.
13. Liu S, Wang B, Yin B, Milner TE, Markey MK, McKinnon SJ, et al. Retinal nerve fiber layer reflectance for early glaucoma diagnosis. *J Glaucoma.* 2014;23:e45–52.
14. Hood DC, Fortune B, Mavrommatis MA, Reynaud J, Ramachandran R, Ritch R, et al. Details of glaucomatous damage are better seen on OCT En face images than on OCT retinal nerve fiber layer thickness maps. *Invest Ophthalmol Vis Sci.* 2015;56:6208–16.
15. Thepass G, Lemij HG, Vermeer KA. Attenuation coefficients from SD-OCT data: structural information beyond morphology on RNFL integrity in glaucoma. *J Glaucoma.* 2017;26:1001–9.
16. Christopher M, Bowd C, Belghith A, Goldbaum MH, Weinreb RN, Fazio MA, et al. Deep learning approaches predict glaucomatous visual field damage from OCT optic nerve head En face images and retinal nerve fiber layer thickness maps. *Ophthalmology.* 2020;127:346–56.
17. Cheloni R, Dewsbery SD, Denniss J. Enhanced objective detection of retinal nerve fiber bundle defects in glaucoma with a novel method for En face OCT slab image construction and analysis. *Transl Vis Sci Technol.* 2021;10:1. <https://doi.org/10.1167/tvst.10.12.1>
18. Cheloni R, Dewsbery SD, Denniss J. A simple subjective evaluation of enface OCT reflectance images distinguishes glaucoma from healthy eyes. *Transl Vis Sci Technol.* 2021;10:31. <https://doi.org/10.1167/tvst.10.6.31>
19. Tan O, Liu L, You Q, Wang J, Chen A, Ing E, et al. Focal loss analysis of nerve fiber layer reflectance for glaucoma diagnosis. *Transl Vis Sci Technol.* 2021;10:9. <https://doi.org/10.1167/tvst.10.6.9>
20. Ashimatey BS, King BJ, Swanson WH. Functional characteristics of glaucoma related arcuate defects seen on OCT en face visualisation of the retinal nerve fibre layer. *Ophthalmic Physiol Opt.* 2021;41:437–46.
21. Alluwimi MS, Swanson WH, Malinovsky VE, King BJ. Customizing perimetric locations based on En face images of retinal nerve fiber bundles with glaucomatous damage. *Transl Vis Sci Technol.* 2018;7:5. <https://doi.org/10.1167/tvst.7.2.5>
22. Vermeer KA, Mo J, Weda JJ, Lemij HG, de Boer JF. Depth-resolved model-based reconstruction of attenuation coefficients in optical coherence tomography. *Biomed Opt Express.* 2013;5:322–37.
23. Girard MJ, Strouthidis NG, Ethier CR, Mari JM. Shadow removal and contrast enhancement in optical coherence tomography images of the human optic nerve head. *Invest Ophthalmol Vis Sci.* 2011;52:7738–48.
24. Vermeer KA, van der Schoot J, Lemij HG, de Boer JF. RPE-normalized RNFL attenuation coefficient maps derived from volumetric OCT imaging for glaucoma assessment. *Invest Ophthalmol Vis Sci.* 2012;53:6102–8.
25. Ashimatey BS, King BJ, Burns SA, Swanson WH. Evaluating glaucomatous abnormality in peripapillary optical coherence tomography enface visualisation of the retinal nerve fibre layer reflectance. *Ophthalmic Physiol Opt.* 2018;38:376–88.
26. Cheung H, Swanson WH. Identifying retinal nerve fiber layer defects using attenuation coefficients. *Invest Ophthalmol Vis Sci.* 2019;60:ARVO E-Abstract 5608.
27. Ashimatey BS, King BJ, Swanson WH. Retinal putative glial alterations: implication for glaucoma care. *Ophthalmic Physiol Opt.* 2018;38:56–65.
28. Delori FC, Gragoudas ES, Francisco R, Pruett RC. Monochromatic ophthalmoscopy and fundus photography. The normal fundus. *Arch Ophthalmol.* 1977;95:861–8.
29. Weiter JJ, Delori FC, Wing GL, Fitch KA. Retinal pigment epithelial lipofuscin and melanin and choroidal melanin in human eyes. *Invest Ophthalmol Vis Sci.* 1986;27:145–52.
30. Ashimatey BS, King BJ, Malinovsky VE, Swanson WH. Novel technique for quantifying retinal nerve fiber bundle abnormality in the temporal raphe. *Optom Vis Sci.* 2018;95:309–17.
31. Clark CA, Elsner AE, Konyonenbelt BJ. Eye shape using partial coherence interferometry, autorefractometry, and SD-OCT. *Optom Vis Sci.* 2015;92:115–22.
32. Girkin CA, Sample PA, Liebmann JM, Jain S, Bowd C, Becerra LM, et al. African descent and glaucoma evaluation study (ADAGES): II. Ancestry differences in optic disc, retinal nerve fiber layer, and macular structure in healthy subjects. *Arch Ophthalmol.* 2010;128:541–50.
33. Knight OJ, Girkin CA, Budenz DL, Durbin MK, Feuer WJ. Effect of race, age, and axial length on optic nerve head parameters and retinal nerve fiber layer thickness measured by cirrus HD-OCT. *Arch Ophthalmol.* 2012;130:312–8.
34. Ho H, Tham YC, Chee ML, Shi Y, Tan NYQ, Wong KH, et al. Retinal nerve fiber layer thickness in a multiethnic normal Asian population: the Singapore epidemiology of eye diseases study. *Ophthalmology.* 2019;126:702–11.
35. Marsh BC, Cantor LB, WuDunn D, Hoop J, Lipyanik J, Patella VM, et al. Optic nerve head (ONH) topographic analysis by stratus OCT in normal subjects: correlation to disc size, age, and ethnicity. *J Glaucoma.* 2010;19:310–8.

SUPPORTING INFORMATION

Additional supporting information can be found online in the Supporting Information section at the end of this article.

How to cite this article: Cheung H, Swanson WH, King BJ. Within-eye and between-subject variability for reflectance of the retinal nerve fibre layer. *Ophthalmic Physiol Opt.* 2022;42:1316–1325. <https://doi.org/10.1111/opo.13027>